Homeotropic surface anchoring of a Gay-Berne nematic liquid crystal

Joachim Stelzer,[1] Lech Longa,[2,*] and Hans-Rainer Trebin[1]
[1]*Institut für Theoretische und Angewandte Physik, Universität Stuttgart, Pfaffenwaldring 57, D-70550 Stuttgart, Germany*
[2]*International Centre of Condensed Matter Physics, Universidade de Brasilia, C.P. 04667-70919-970 Brasilia, DF, Brazil*
(Received 13 December 1996)

The ordering of a nematic liquid crystal in the presence of a smooth surface is analyzed in detail. In particular, the force constants for homeotropic anchoring are estimated by a local density functional method with data from molecular dynamics simulations. The system studied is a model Gay-Berne nematic liquid crystal. For the molecule-surface interaction both an anisotropic and an isotropic one-particle potential are taken. In both cases a surface-induced smectic *A* phase is being observed even though the phase is unstable in the bulk. [S1063-651X(97)02206-X]

PACS number(s): 61.30.Cz, 64.70.Md, 05.70.Ce, 62.20.Dc

Surfaces of nematic liquid crystals show a rich variety of ordered states [1]. With respect to positional order smectic or even crystalline layers of the molecules may form. Concerning orientational order the long molecular axes may be anchored along one or along several discrete directions, or along a continuous set of directions.

With the help of anchoring conditions one can tailor the director field in the bulk of a nematic liquid crystal such that the polarization plane of light is guided according to wish for display purposes.

Anchoring is achieved by a suitable preparation of the cover glasses for the nematic cell, and although a myriad of glasses is being prepared by empirical recipes annually, the underlying microscopic mechanisms of anchoring are not yet fully understood.

Phenomenologically, anchoring is described by a surface potential or anchoring free energy, which depends on the surface director $\hat{\boldsymbol{n}}$. For an anchoring configuration cylindrically symmetric about a preferred direction $\hat{\boldsymbol{n}}_p$, the potential most frequently used is of the Rapini and Papoular form [2],

$$\mathcal{F}_{\mathrm{anch}}=\tfrac{1}{2}c_\theta \sin^2(\theta-\theta_p)\equiv\tfrac{1}{2}c_\theta[1-(\hat{\boldsymbol{n}}\cdot\hat{\boldsymbol{n}}_p)^2], \qquad (1)$$

where θ and θ_p are the polar angles of $\hat{\boldsymbol{n}}$ and $\hat{\boldsymbol{n}}_p$, respectively.

Alternatively one can expand the surface potential into a series of Legendre polynomials

$$\mathcal{F}_{\mathrm{anch}}=W_2P_2(\hat{\boldsymbol{n}}\cdot\hat{\boldsymbol{n}}_p)+W_4P_4(\hat{\boldsymbol{n}}\cdot\hat{\boldsymbol{n}}_p)+\cdots. \qquad (2)$$

The coefficients W_2, W_4, and $c_\theta=-3\,W_2-10\,W_4$ of the expansions (1) and (2), denoted anchoring strengths, must depend both on the properties of the equilibrium bulk nematic liquid crystal and on the way the surface interacts with the bulk. They have been determined experimentally [3,4]. Theories about the surface-bulk interaction with the introduction of a phenomenological anchoring free energy were developed by Sluckin and Poniewierski [5], by Sen and Sullivan [6], and by Osipov and Hess [7]. Theoretical estimates of the anchoring strengths were performed by Tjipto-Margo and Sullivan [8], yielding rough limits for the ratio W_2/W_4.

This paper is devoted to a microscopic study of surface-induced ordering in nematic liquid crystals due to homeotropic anchoring. The strength of the nematic ordering on the surface is estimated by the Rapini-Papoular constants. These are found by combining molecular dynamics simulations at constant density (pressure) and temperature with a local density functional approach. The pair interaction of the rodlike molecules was modeled by the anisotropic Gay-Berne potential [9]. For the interaction of a molecule with the surface, first an anisotropic potential was taken which favors an alignment along the surface normal. The equations for translational and rotational motion of a system of 1053 particles were solved numerically. We not only observe stable homeotropic anchoring, but also surface-induced smectic *A* layers, which penetrate into the bulk with a temperature dependent coherence length. From the molecular data the pair distribution function (PDF) was extracted and converted into the direct correlation function (DCF) by an iterative solution of the Ornstein-Zernike integral equation. Finally, relations were derived between the surface anchoring strengths and structural quantities like the DCF. This allows us to estimate the temperature variation of surface anchoring.

In the molecular dynamics simulations the rodlike molecules are specified by a set of positions $\boldsymbol{r}_i$, unit vectors $\hat{\boldsymbol{e}}_i$ for the orientations, velocities $\boldsymbol{v}_i$, and angular velocities $\boldsymbol{\omega}_i$. The phase diagram of particles interacting by the Gay-Berne potential has been determined by de Miguel *et al.* [10]. We have used the same anisotropy parameters and have performed the simulations within the temperature and density range of the stable nematic phase.

The starting point for surface simulations was a nematic bulk phase in equilibrium, subject to periodic boundary conditions. We generated it in bulk simulations (no surfaces

*Permanent address: Department of Statistical Physics, Jagiellonian University, Reymonta 4, Kraków, Poland. Electronic address: lechifuj@jetta.if.uj.edu.pl

 © 1997 The American Physical Society

present) by melting a tetragonal crystal of rods perfectly aligned along the z axis. The nematic output configuration was increased twice along the z axis to avoid finite size effects during the surface simulation. The surface potentials were adjusted to the top and bottom of this enlarged nematic at $z_0 = \pm z_{\rm surf}$. For simplicity, each surface was modeled on a molecular level through a one-dimensional, one-particle Lennard-Jones potential in z direction. The depth of the potential was taken angle dependent, favoring a molecular alignment along the surface normal (z axis). For this purpose we applied a prefactor $\epsilon(\hat{\boldsymbol{e}}_i, \hat{\boldsymbol{e}}_j, \hat{\boldsymbol{r}}_{ij})$ as in the Gay-Berne potential where $\hat{\boldsymbol{e}}_j$ was identified with $\hat{\boldsymbol{z}}$ and $\hat{\boldsymbol{r}}_{ij}$ with $\hat{\boldsymbol{x}}$:

$$V_i^{\rm surf} = 4\,\epsilon(\hat{\boldsymbol{e}}_i, \hat{\boldsymbol{e}}_j = \hat{\boldsymbol{z}}, \hat{\boldsymbol{r}}_{ij} = \hat{\boldsymbol{x}}) \left[\left(\frac{\sigma_0}{z_i - z_0} \right)^{12} - \left(\frac{\sigma_0}{z_i - z_0} \right)^{6} \right]. \quad (3)$$

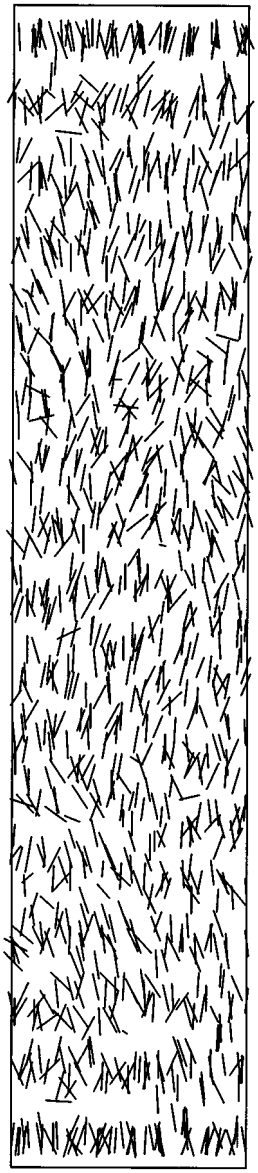

FIG. 1. A typical configuration of Gay-Berne particles in the nematic phase with a surface-induced smectic A phase for nonzero surface anchoring. Parameters (in reduced units) are temperature $T = 1.10$, pressure $P = 4.5$, volume density $\rho = 0.33$, surface density $\sigma = 0.43$.

For an equilibrium period of 20 000 time steps (time step 10^{-3} in reduced units [11]) the positions $\pm z_{\rm surf}$ of the surfaces were left free to move along the z direction in order to adjust the pressure to its bulk nematic value, corresponding to a density of 0.33 (in reduced units) and the temperature values of the phase diagram [10]. Afterwards, the walls were fixed for other 40 000 time steps, to evaluate the time averages of the interesting quantities. During simulations the director was parallel to the z axis. The box dimensions were equal to $8.69 \times 8.69 \times 32.9$ in reduced Gay-Berne units [11].

A snapshot of the molecular dynamics run (Fig. 1) reveals top and bottom layers of homeotropic anchoring. Interestingly, *the surfaces have induced a smectic A phase* penetrating into the bulk with a temperature dependent coherence length. Such a phase is not present in the bulk phase diagram of de Miguel *et al.* [10].

Figures 2 and 3 display the x-y integrated density profile for two different temperatures in the nematic range of the Gay-Berne phase diagram [10]. The number of the layers and the coherence length decrease linearly with growing temperature. Surface-induced smectic A phases have been observed experimentally by x-ray scattering under glancing angles [12,13]. Coherence lengths of about 100 Å have been measured, corresponding to about three to six smectic layers as in our simulations.

During the molecular dynamics runs, temperature, pressure, and nematic director were monitored. For the calculation of the anchoring strengths the order parameters, i.e., averaged values of the Legendre polynomials $P_n : \langle P_n \rangle = \langle (1/N) \Sigma_i P_n[\cos(\hat{\boldsymbol{e}}_i \cdot \hat{\boldsymbol{n}})] \rangle$, and the angle dependent pair distribution function $g(\boldsymbol{r}_i, \boldsymbol{r}_j, \boldsymbol{\Omega}_i, \boldsymbol{\Omega}_j)$ were evaluated. The latter was processed as an expansion into spherical harmonics [14].

Now we turn to the estimates of the Rapini-Papoular coefficients. This is performed by calculating the Helmholtz free energy difference $\Delta\mathcal{F}$ between deformed and undeformed equilibrium nematic states characterized by distributions $\rho_d(\mathbf{1})$ and $\rho_u(\mathbf{1})$, respectively, where $(\mathbf{1}) \equiv (\boldsymbol{r}_1, \boldsymbol{\Omega}_1)$. To second order in the density difference $\delta\rho = \rho_d - \rho_u$ the expression for $\Delta\mathcal{F}$ may be written as [15]

$$\begin{aligned} \beta\Delta\mathcal{F} &= \beta\mathcal{F}[\rho_d] - \beta\mathcal{F}[\rho_u] \\ &= \int \rho_d(\mathbf{1}) \ln \frac{\rho_d(\mathbf{1})}{\rho_u(\mathbf{1})} d(\mathbf{1}) - \int \delta\rho_d(\mathbf{1}) d(\mathbf{1}) \\ &\quad - \frac{1}{2!} \int \int c(\mathbf{1}, \mathbf{2}, [\rho_u])\, \delta\rho(\mathbf{1})\, \delta\rho(\mathbf{2}) d(\mathbf{1}) d(\mathbf{2}), \end{aligned} \quad (4)$$

where c is the direct pair correlation function of the undeformed confined nematic, $d(\mathbf{1}) = d\boldsymbol{r}_1 d\boldsymbol{\Omega}_1$, β is the inverse temperature, and $\int d(\mathbf{1}) \rho(\mathbf{1}) = N$, where N is the number of particles.

The anchoring free energy can be extracted from the expansion (4) after a few simplifications. First of all we choose to treat slowly varying distorted director fields

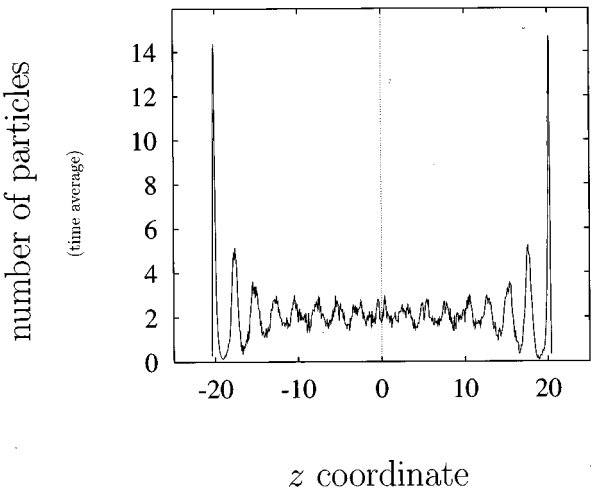

FIG. 2. The x-y integrated density profile (in reduced units) of the nematic phase in the presence of surface anchoring. Parameters (in reduced units) are temperature $T=1.00$, pressure $P=4.35$, volume density $\rho=0.33$, surface density $\sigma=0.44$.

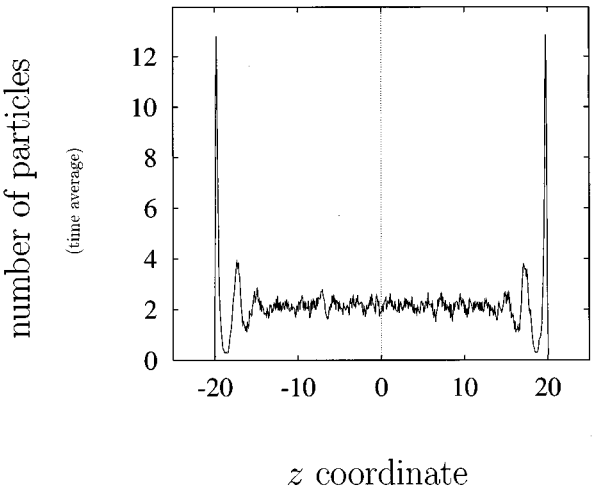

FIG. 3. The x-y integrated density profile (in reduced units) of the nematic phase in the presence of surface anchoring. Parameters (in reduced units) are temperature $T=1.50$, pressure $P=4.8$, volume density $\rho=0.33$, surface density $\sigma=0.40$.

$\hat{\boldsymbol{n}}_d(\boldsymbol{r})[\hat{\boldsymbol{n}}_d(\boldsymbol{r})\equiv\hat{\boldsymbol{n}}(\boldsymbol{r})]$ and assume that the free energy func--tional is locally in equilibrium. This is equivalent to the mathematical simplification, widely used in the literature [16], that $\rho_d(\mathbf{1})=\rho_u[\boldsymbol{r},\hat{\boldsymbol{n}}(\boldsymbol{r})\cdot\boldsymbol{\Omega}]$. Also we restrict (as in simulations) to smooth planar surfaces parallel to the x-y plane which implies that $\rho_u[\boldsymbol{r},\hat{\boldsymbol{n}}(\boldsymbol{r})\cdot\boldsymbol{\Omega}]=\rho_u[z,\hat{\boldsymbol{n}}(z)\cdot\boldsymbol{\Omega}]$ and $\rho_u[\boldsymbol{r},\hat{\boldsymbol{n}}_u(\boldsymbol{r})\cdot\boldsymbol{\Omega}]=\rho_u[z,\hat{\boldsymbol{n}}_u\cdot\boldsymbol{\Omega}]$ [$\hat{\boldsymbol{n}}_u=\hat{\boldsymbol{n}}_p=\hat{\boldsymbol{z}}$ stands for the un--distorted equilibrium director field and $\hat{\boldsymbol{n}}(z)$ represents the surface-induced distortion of the director field].

The third approximation is based on the gradient expansion of the one-particle distribution functions $\rho_u(\boldsymbol{r}_2,\boldsymbol{\Omega}_2)=\rho_u(\boldsymbol{r}_1,\boldsymbol{\Omega}_2)+(\boldsymbol{r}_{12}\cdot\nabla)\rho_u(\boldsymbol{r}_1,\boldsymbol{\Omega}_2)+\cdots$ in Eq. (4).

With all of the above, microscopic expressions for various elastic constants are now easily inferred from Eq. (4). For example, the Poniewierski and Stecki expressions [17] for the Frank elastic constants are given by the gradient terms. The anchoring free energy per unit area is given by the terms that do not involve gradients. Excluding the ideal gas part it reads

$$\beta\mathcal{F}_{\mathrm{anch}}=\int\rho_0^2 f[z,\hat{\boldsymbol{n}}(z),\hat{\boldsymbol{n}}_p]dz$$
$$=-\frac{1}{2}\int\rho_0^2 dz\int d\boldsymbol{\Omega}\,\delta P(z,\boldsymbol{\Omega})\,\delta P(z,\boldsymbol{\Omega}')\int\int\int\int c(x-x',y-y',z,z',\boldsymbol{\Omega},\boldsymbol{\Omega}',[\hat{\boldsymbol{n}}_p])dx'dy'dz'd\boldsymbol{\Omega}', \qquad (5)$$

where ρ_0 denotes the volume particle density and $P=\rho_u/\rho_0$ is the one-particle distribution function. Please note that $\hat{\boldsymbol{n}}(z)$ in Eq. (5) relaxes from its surface value $\hat{\boldsymbol{n}}\equiv\hat{\boldsymbol{n}}(0)$ to $\hat{\boldsymbol{n}}_p$ in a thin layer (Δz) located above the surface. Hence the integration over z in Eq. (5) is, in practice, restricted to the interval Δz.

In order to convert the expressions (5) into the Rapini-Papoular form (2) we expand the orientationally dependent functions into spherical harmonics:

$$\int\int c(\cdots)dx'dy'=4\pi\sum_{l_1l_2l}^{\text{even}}c_{l_1l_2l}(z,z')\sum_{m_1m_2m}\left(\begin{smallmatrix}l_1 l_2\\ m_1 m_2\end{smallmatrix}\middle|\,l_m\right)Y^{l_1}_{m_1}(\boldsymbol{\Omega}_1)Y^{l_2}_{m_2}(\boldsymbol{\Omega}_2)Y^{l}_{m}{}^{*}(\hat{\boldsymbol{n}}_p),$$

$$P(z,\hat{\boldsymbol{m}}_\alpha\cdot\boldsymbol{\Omega}_1)=\sum_{l'}^{\text{even}}\langle P_{l'}\rangle(z)\sum_{m'}Y^{l'}_{m'}{}^{*}(\boldsymbol{\Omega}_1)Y^{l'}_{m'}(\hat{\boldsymbol{m}}_\alpha),$$

$$\alpha=0,1 \quad (6)$$

where the abbreviation $(^{l_1 l_2}_{m_1 m_2}|^{l}_{m})$ is used for the Clebsch-Gordan coefficients, $\hat{\boldsymbol{m}}_0=\hat{\boldsymbol{n}}(z)$, and $\hat{\boldsymbol{m}}_1=\hat{\boldsymbol{n}}_p$. This allows us to perform analytically the integrations over all solid angles reducing the anchoring energy to an infinite series. If we additionally replace $\langle P_l\rangle(z)$ by their averaged values $\langle P_l\rangle$ and assume that $\hat{\boldsymbol{n}}(z)$ equals $\hat{\boldsymbol{n}}_p$ except for $0\leqslant z\leqslant\Delta z$ [where $\hat{\boldsymbol{n}}(z)=\hat{\boldsymbol{n}}(0)\equiv\hat{\boldsymbol{n}}$] then

$$\beta\mathcal{F}_{\mathrm{anch}}\approx-\frac{4\pi\rho_0\sigma_0}{2}\sum_{l_1 l_2 l}^{\mathrm{even}}\langle P_{l_1}\rangle\langle P_{l_2}\rangle\left[\int dz' c_{l_1 l_2 l}(0,z')\right]$$
$$\times\sum_{m_1 m_2 m}(^{l_1 l_2}_{m_1 m_2}|^{l}_{m})\sum_{\alpha,\beta=0,1}(-1)^{\alpha+\beta}Y^{l_1}_{m_1}$$
$$\times(\hat{\boldsymbol{m}}_\alpha)Y^{l_2}_{m_2}(\hat{\boldsymbol{m}}_\beta)Y^{l*}_{m}(\hat{\boldsymbol{n}}_p). \tag{7}$$

Here $\sigma_0=\rho_0\Delta z$ is the lateral particle density in the molecular layer closest to the surface. It should also be noted that the terms involving sums over m_1, m_2, and m are spherical invariants of $\hat{\boldsymbol{n}}$ and $\hat{\boldsymbol{n}}_p$ and hence proportional to $P_l(\hat{\boldsymbol{n}}\cdot\hat{\boldsymbol{n}}_p)$. Gathering these terms together and comparing with the definition of the macroscopic anchoring energy (2) yields immediately the microscopic expressions for the surface anchoring strengths W_l. These expressions are consistent with the observation that the Rapini-Papoular surface anchoring takes place in a thin layer close to the surface. The ''range of the anchoring'' is determined by the short-range behavior of the direct pair correlation.

The central quantity entering Eq. (7) is the temperature and density dependent direct pair correlation function $c(\mathbf{1},\mathbf{2})$ for the *undeformed, equilibrium confined system*. It is related to the numerically determined pair distribution function g or pair correlation function $h\equiv g-1$ via the Ornstein-Zernike equation [15]

$$h(\mathbf{1},\mathbf{2})=c(\mathbf{1},\mathbf{2})+\int d(\mathbf{3})c(\mathbf{1},\mathbf{3})\rho_u(\mathbf{3})h(\mathbf{3},\mathbf{2}). \tag{8}$$

Although, in principle, the correlation function h could be determined from simulations to an arbitrary degree of accuracy, reliable calculations of c from Eq. (8) for confined systems do not seem feasible at present. Hence, in order to make the numerical estimates of the Rapini-Papoular constants possible, we are forced to perform a series of simplifications in Eq. (8). First of all we impose translational symmetry on h and c in Eq. (8) and restrict to the terms with $l_1,l_2\leqslant 4$ in their spherical harmonic expansions. Next, the one-particle orientational distribution function $\rho_u(\boldsymbol{r},\boldsymbol{\Omega})$ is replaced by its isotropic form $\rho_0/4\pi$. The usefulness of this approximation in the description of ordered nematics as well as all technical details concerning simulations have been discussed thoroughly in recent publications [14,18].

The approximations applied to the Ornstein-Zernike equation also simplify the anchoring energy, Eq. (7). Now it reads

$$\beta\mathcal{F}_{\mathrm{anch}}=\sum_{l}^{\mathrm{even}}\left[\sqrt{\frac{2l+1}{4\pi}}\rho_0\sigma_0\langle P_l\rangle^2\int dr r^2 c_{ll0}(r)\right]$$
$$\times[P_l(\hat{\boldsymbol{n}}\cdot\hat{\boldsymbol{n}}_p)-1], \tag{9}$$

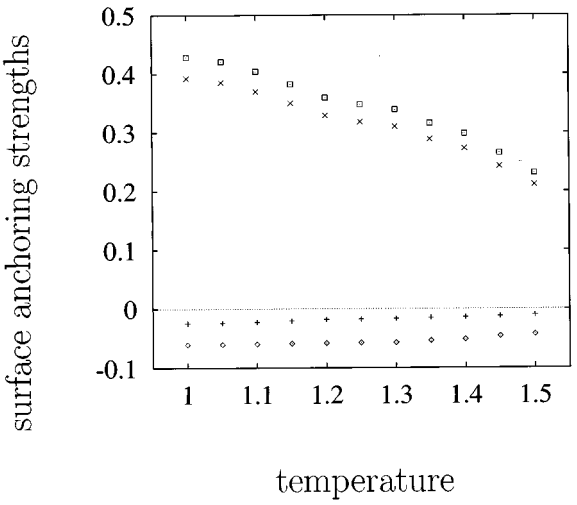

FIG. 4. The temperature dependence of the anchoring strengths (in reduced units). Parameters (in reduced units) and symbols are pressure $P=4.35-4.8$, volume density $\rho=0.33$, surface density $\sigma=0.44-0.40$; rhombi: W_2, crosses: W_4, squares: c_θ (anisotropic), $\times$ symbols: c_θ (isotropic surface).

where $c_{ll0}(r)$ are the spherical harmonic expansion coefficients of the DCF.

A direct comparison of the series (9) with the definition of the macroscopic anchoring energy (2) yields the microscopic expressions for the leading surface anchoring strengths W_2 and W_4. The surface density σ_0 entering Eq. (9) is computed with the same accuracy as the bulk density ρ_0 by averaging the number of particles in the monolayer closest to the surface over the production run of the molecular dynamics (MD) simulation and dividing this average number of particles by the x-y cross section of the simulation box.

We have studied how the anisotropy of the molecule-surface interaction influences the anchoring strengths by performing two independent molecular dynamics series. The first one is based on the ''anisotropic'' surface potential (3), where surface and bulk Gay-Berne parameters were taken equal. In the second series we took an ''isotropic'' surface potential, with the ground state energy ϵ independent of the molecular orientations. For both types of surfaces the Rapini-Papoular constant differed by less than 10% (Fig. 4). In both cases we observed surface-induced smectic A layering and found that the numerical values of W_2 depend on the number of surface-induced smectic layers. Similar correlations have recently been suggested by Li and Lavrentovich [4].

We would like to mention that the possibility of inducing smectic ordering due to the presence of restricting surfaces strongly depends on the form of the surface potential. Recently Zhang *et al.* [19] simulated basically the same system, but with a surface potential that favors planar alignment, and they found no smectic layering. We have also performed other series of MD simulations for generalized anchoring directions [20]. The smectic layers, although always present, were less pronounced in these cases.

In connection with the above results it seems important to comment on the form of the potential we used in our simulations to describe the interaction between a liquid crystal molecule and the surface. One perhaps would expect that the surface-bulk interaction should be modeled by the conven-

tional 9-3 surface potential (obtained by integrating the 12-6 Lennard-Jones potential over all positions of one molecule in the substrate) instead of the 12-6 form we used. In reality, however, neither 9-3 nor 12-6 potentials provide a good parametrization of the real surfaces that anchore nematics (see, e.g., [1,3], and references therein). For a given bulk nematic phase and for fixed temperature and pressure various anchorings could be realized in practice. The primary difference between them is the coherence length of the induced smectic *A* layering. As the proposed theory of anchoring emphasizes the rôle of the structure of the system one may expect that all surface potentials generating (for fixed temperature and pressure) a smectic *A* ordering of the same coherence length should yield similar anchoring strengths. This has actually been proven by our simulations.

Furthermore, experimental investigations of the surface-induced smectic *A* layering in nematics indicate that such effects are present on a length scale of 100–200 Å. This fits well to our simulations. Thus, in order to establish a simple model of short-range surface interaction, we chose the 12-6 Lennard-Jones parametrization. The 9-3 surface potential would give rise to a quite long-range surface-induced smectic *A* ordering which (as far as we can say) has not been reported so far.

The detailed temperature variation of the surface anchoring strengths is displayed in Fig. 4. We found that the absolute values of the constant W_4 are about half an order of magnitude smaller than those of W_2. Similar estimates for the ratio W_4/W_2 have been obtained previously by Osipov and Hess [7] for a liquid-vapor interface. Thus the calculations reveal a rapid convergence of the expansion for the anchoring energy (2). Due to the negative values of W_2 and W_4 the Rapini-Papoular constant c_θ is positive. Hence the homeotropic anchoring yields a stable configuration for the Gay-Berne nematic, i.e., the anchoring energy (2) has its absolute minimum at the preferred orientation $\theta_p=0$. Comparing the surface anchoring strengths with the bulk elastic constants of recent calculations [14] (both in reduced units [11] and for the same Gay-Berne nematic states) we find that the former are about an order of magnitude smaller.

The ratios of the Rapini-Papoular constant to the bulk elastic constants have been measured experimentally [3]. Although there is a wide discrepancy among the various results for W_2, sometimes by two orders of magnitude, it seems that most of them are within a range between 10^{-5} N/m and 10^{-6} N/m. Considering typical values for the bulk elastic constants $K=10^{-12}$ N and a thickness of 10^{-6} m for the liquid crystal cell, the results of our simulations for the ratio c_θ/K are at the lower edge of the experimental data.

Finally, unlike former calculations of surface anchoring performed by Tjipto-Margo and Sullivan [8] and by Osipov and Hess [7] that only treated liquid-vapor interface, we have taken into account the interaction between the nematic and an anisotropic solid substrate on a microscopic level. The theory elaborated here correlates the anchoring strengths with structural quantities. The direct correlation function has been gained by solving the Ornstein-Zernike integral equation. The pair distribution function which enters this equation has been determined from the molecular dynamics simulations. Emphasizing the dependence on the structure seems important for a correct interpretation of the anchoring in terms of microscopic quantities. Most probably this is the reason why our dimensionless ratio c_θ/K is in line with experimental results, even though the interaction potential used is relatively simple. As the Ornstein-Zernike equation could be solved with controlled approximations this seems to give an estimate of *absolute* values of the Rapini-Papoular constants, not just their ratios as in all previous treatments.

One of the authors (L.L.) thanks Dr. M. A. Osipov for stimulating discussions. This work was supported by the Deutsche Forschungsgemeinschaft (DFG) under Grant No. Tr 154/7-2, by the CNPQ Committee in Brazil and by the European Community under Grant No. ERBCIP-DCT940607.

[1] B. Jérôme, Rep. Prog. Phys. **54**, 391 (1991).
[2] A. Rapini and M. Papoular, J. Phys. (France) Colloq. **30**, C4-54 (1969).
[3] L. M. Blinov, A. Y. Kabayenkov, and A. A. Sonin, Liq. Cryst. **5**, 645 (1989); D.-F. Gu, S. Uran, and C. Rosenblatt, *ibid.* **19**, 427 (1995).
[4] For comparison between the anchoring strength of smectics *A* and nematics see Z. Li and O. D. Lavrentovich, Phys. Rev. Lett. **73**, 280 (1994).
[5] T. J. Sluckin and A. Poniewierski, in *Fluid Interfacial Phenomena*, edited by C. A. Croxton (Wiley, New York, 1986).
[6] A. K. Sen and D. E. Sullivan, Phys. Rev. A **35**, 1391 (1987).
[7] M. Osipov and S. Hess, J. Chem. Phys. **99**, 4181 (1993).
[8] B. Tjipto-Margo and D. E. Sullivan, J. Chem. Phys. **88**, 6620 (1988).
[9] J. G. Gay and B. J. Berne, J. Chem. Phys. **74**, 3316 (1981).
[10] E. de Miguel, L. F. Rull, M. K. Chalam, and K. E. Gubbins, Mol. Phys. **74**, 405 (1991).
[11] M. P. Allen and D. J. Tildesley, *Computer Simulations of Liquids* (Oxford Science Publications, Oxford, 1987).
[12] J. Als-Nielsen, F. Christensen, and P. S. Pershan, Phys. Rev. Lett. **48**, 1107 (1982).
[13] E. F. Gramsbergen and W. H. de Jeu, J. Phys. (France) **49**, 363 (1988).
[14] J. Stelzer, L. Longa, and H.-R. Trebin, Mol. Cryst. Liq. Cryst. **262**, 455 (1995); J. Chem. Phys. **103**, 3098 (1995); and to be published.
[15] See, e.g., J. P. Hansen and I. R. Mc Donald, *Theory of Simple Liquids*, 2nd ed. (Academic Press, London, 1986).
[16] See, e.g., A. M. Somoza and P. Tarazona, Mol. Phys. **72**, 911 (1991).
[17] A. Poniewierski and J. Stecki, Mol. Phys. **38**, 1931 (1979).
[18] M. P. Allen, C. P. Mason, E. de Miguel, and J. Stelzer, Phys. Rev. E **52**, R25 (1995).
[19] Z. Zhang, A. Chakrabarti, O. G. Mouritsen, and M. J. Zuckerman, Phys. Rev. E **53**, 2461 (1996).
[20] J. Stelzer, P. Galatola, G. Barbero, and L. Longa, Phys. Rev. E **55**, 477 (1997).